

# Physical Aspects of Rapid Cyclogenesis in the Gulf of Alaska

By JAY S. WINSTON, Extended Forecast Section, U.S. Weather Bureau, Washington, D.C.

(Manuscript received October 5, 1954)

## *Abstract*

The Gulf of Alaska is often the site of rapid development of large-scale cyclonic activity which can have profound effects on the long-wave pattern over North America in a matter of 24 to 48 hours. During much of the year such cyclogenesis takes place in the presence of a large heat source associated with rapid modification of cold Arctic air masses moving from Alaska out over the warmer sea surface of the Gulf. In order to get some insight into the mechanism of cyclogenesis under these special conditions a case of intense development occurring early in February 1950 has been studied, mainly in terms of the vorticity equation. The effects of barotropic redistribution of vorticity seem to account for much of the development. However, it is found that there exist pronounced fields of divergence and vertical motion, which particularly at the time of most rapid development reflect the influence of heat sources on the circulation.

## **1. Introduction**

The Gulf of Alaska is frequently the site of rapid development of intense cyclonic activity. Much of this cyclogenesis occurs on such a large scale that the basic planetary wave pattern is often radically altered in a few days, especially downstream over North America and the Atlantic. The synoptic aspects of a frequent type of trough development in the Gulf of Alaska and its importance in changing the long-wave pattern over broad areas of the Northern Hemisphere were recognized at an early stage in extended forecasting practice (NAMIAS and CLAPP, 1944). Namias has attributed this type of trough intensification in the area to the rapid modification of cold Arctic air masses which are advected over the open water surface of the Gulf in the northerly flow to the east of a ridge situated over the Bering Sea or the northeast Siberian peninsula. The rapid addition of heat and moisture to the frigid air striking the relatively warm waters of the Gulf was postulated to lead to widespread, organized convection and horizontal convergence, thereby creating sufficient cy-

clonic vorticity to produce a deep trough. However, this sequence of events depends on the initial establishment of the upstream ridge and the associated northerly current to its east which directs the flow of Arctic air over the Gulf. Since this ridge frequently appears to be formed by the barotropic redistribution of absolute vorticity, it is likely that barotropic effects are also influential in cyclogenesis in the Gulf of Alaska.

These qualitative considerations give some ideas about the physical processes at work in such cyclogenesis, and indeed these concepts have been extremely useful in making many successful medium- and long-range forecasts. However, knowledge of the influence of heat sources on changes in circulation is at best extremely limited, and the quantitative determination of these effects, especially in relation to other dynamic processes, is still in its early stages. Recently SMAGORINSKY (1953) calculated the dynamical influence of large-scale heat sources on the steady-state mean motions and found that these account for some of the gross features of the monthly normal circula-

tion patterns at sea level and in mid-troposphere. Also, recent attempts to make numerical predictions for medium-range time periods have included some indirect estimates of the influence of heat sources (CLAPP, 1953). The effects of non-adiabatic heating have been virtually neglected, however, in short-range prediction methods. For example, SUTCLIFFE (1947) made the adiabatic assumption in order to simplify the use of thickness patterns for prediction of development arising from the baroclinic nature of the atmosphere. Even in the increasingly complex numerical prediction models heating effects have not as yet been incorporated although it has been suggested that they may be taken into account without serious numerical complication (cf., CHARNEY and PHILLIPS, 1953). In those cases which have thus far been subjected to numerical calculation the adiabatic assumption has apparently proved to be satisfactory since some rather good predictions of severe storm developments have been made. Up to now, however, there is little evidence that the application of adiabatic models can be markedly successful in cases of explosive cyclogenesis where large heat sources are involved, as in the Gulf of Alaska.

The main reason for the neglect of heat sources in quantitative methods of prediction stems from the woeful lack of precise knowledge of heating at any given time. In evaluating turbulent transfer of heat from a warmer water surface to colder air (the process which is presumably most important in the Gulf of Alaska) one might attempt to use the type of equation employed by JACOBS (1951), which depends on an assumed heat exchange coefficient and the temperature difference between sea and air. But there is generally insufficient information about these quantities to attempt to compute heating on a day-to-day synoptic basis thereby. As an alternative, heating can probably be calculated to a reasonably good approximation from the three-dimensional field of motion itself, but unless vertical motion can be computed independently of the vorticity and energy equations the consideration of heat sources in a numerical prediction scheme is immediately precluded. Obviously this poses a knotty problem.

Nevertheless before delving into such difficult questions it is desirable to learn more about how heat sources influence circulation

changes and just how important these effects are. The Gulf of Alaska region in the cold season provides a good testing ground in that heat sources are large and cyclonic development is often quite explosive. If heating is of importance then surely its effects should be apparent on circulation developments in this locale. In order to get some further insight then into the mechanism of development associated with a large heat source, a case of intense cyclonic development in early February 1950 was chosen for detailed study. The quantitative approach in this work concentrates mainly on the vorticity equation, because of its usefulness in numerical prediction work and its ready adaptability to the geostrophic approximation, a practical necessity with the data available over the Gulf of Alaska region.

## 2. Broad-scale features of cyclogenesis

The broad-scale circulation changes associated with intense cyclonic development over the Gulf of Alaska in early February 1950 are portrayed clearly by the series of 5-day mean 700-mb charts at one-half week intervals shown in Fig. 1. Note how the Gulf of Alaska trough developed in conjunction with the retrogression to the central Aleutians and the Bering Sea of a large ridge originally in the eastern Aleutians. This resulted in northerly flow of cold air over the Gulf of Alaska. The trough in the Gulf of Alaska was essentially a new perturbation since the initial broad northerly flow east of the large ridge split into two by the period, February 1—5, while the subpolar low over eastern Canada maintained and moved eastward. In other words, the downstream half wave length between ridge and trough was shortened in a discontinuous fashion as the Gulf of Alaska trough developed. Farther south over the United States similar radical changes in circulation took place. Prior to Gulf of Alaska trough development a broad cyclonic flow, associated with the trough extending southwestward from the Canadian low, dominated western and central sections of the United States with attendant storminess and cold weather in the west. With the establishment of the trough extending southward from the Gulf of Alaska heights rose rapidly, anti-cyclonic circulation developed, and consequently more moderate weather set in over the western United States. Such substantial adjust-

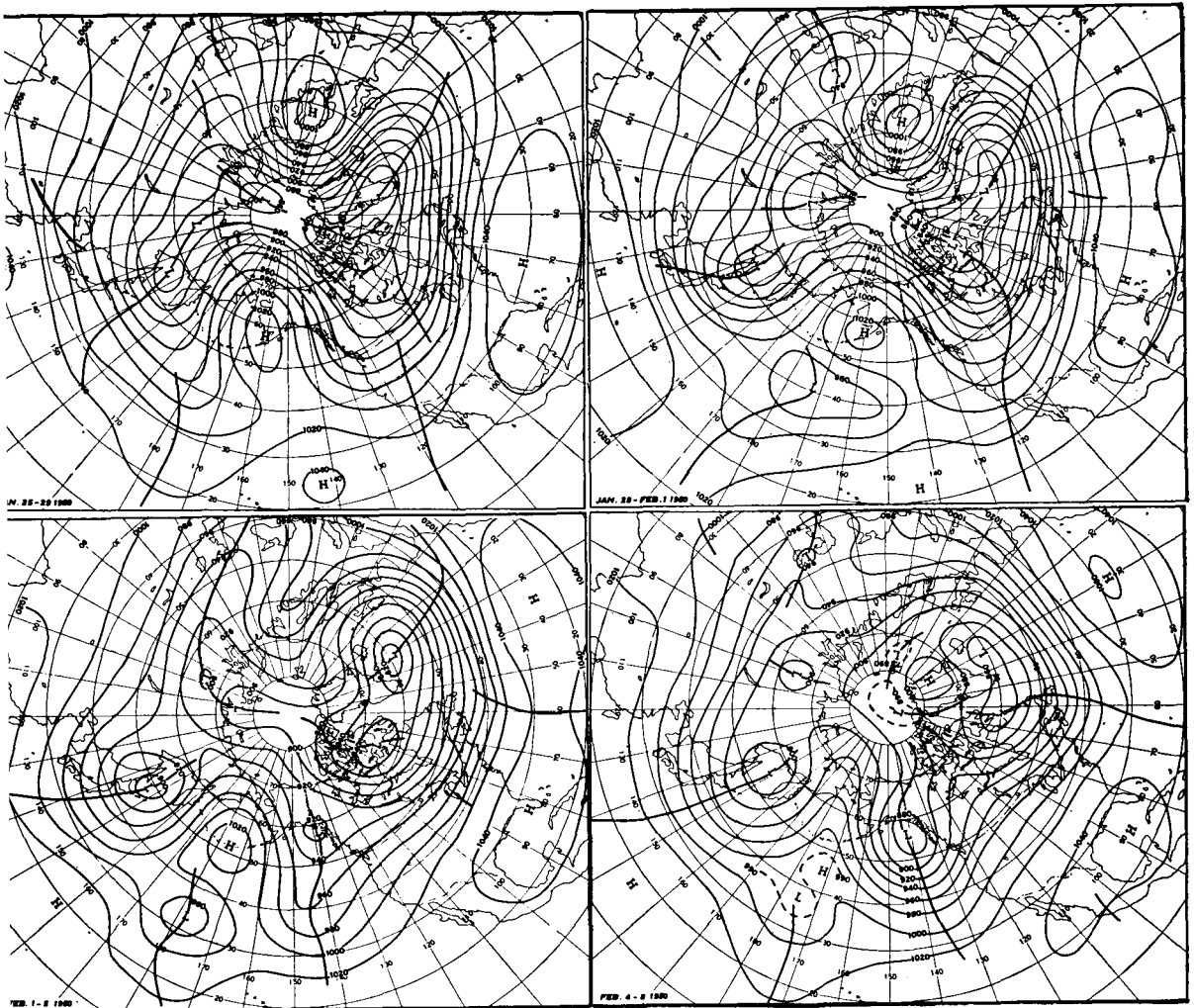


Fig. 1. Series of 5-day mean 700-mb charts illustrating large-scale aspects of strong cyclonic development in the Gulf of Alaska. Charts are at twice-weekly intervals beginning with period January 25—29, 1950. Trough lines are indicated by heavy solid lines; contours in tens of geopotential feet.

ments in circulation over North America are rather typical following rapid cyclogenesis over the Gulf of Alaska.

It has already been pointed out that trough development in this case was apparently dependent upon retrogression of the ridge over the Aleutians and the Bering Sea. The westward motion of this ridge in turn appears to be related to at least two other developments in the western and central Pacific which are evident in Fig. 1. One was the intensifying southerly flow in the vicinity of Kamchatka

beginning in the period January 28—February 1 as compared with January 25—29. The other was the closed low in the central Pacific at lower latitudes which was most intense in the period January 28—February 1. Qualitatively it appears that barotropic vorticity flux from both the broad southeasterly current north of this closed low and the increasing southerly current east of Japan played a major role in the retrogression of the ridge over the Bering Sea, and consequently in the subsequent development of the Gulf of Alaska trough.

The sequence of events following the establishment of strong southerly flow at a longitude farther west than previously in the western Pacific is portrayed somewhat more clearly by a time-longitude chart (Fig. 2). This chart shows the variation of meridional components of the 5-day mean geostrophic wind at 700 mb along

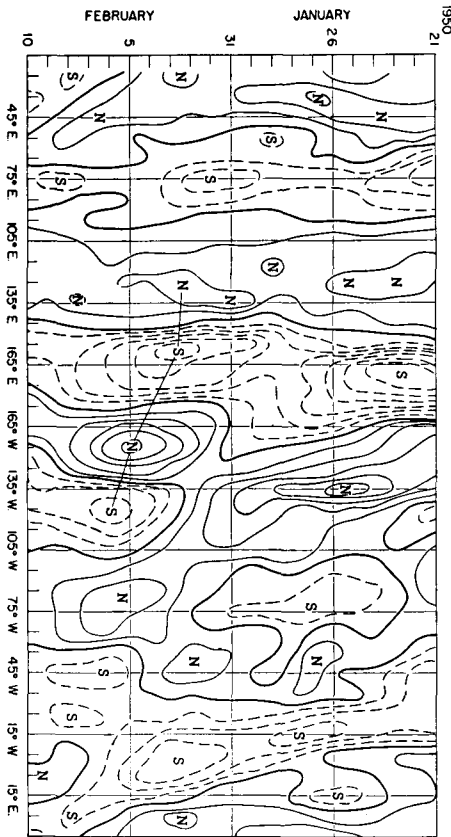


Fig. 2. Time-longitude chart of meridional components of 5-day mean geostrophic wind at 700 mb along the 50°N latitude circle. Isoleths of constant wind speed are drawn at intervals of 100 feet of height difference over 10° of longitude (i.e., approximately at intervals of 3.7 m/sec) with dashed lines showing southerly flow and solid lines northerly flow. Dark solid lines represent zero values of meridional flow and generally mark positions of troughs and ridges.

the 50° N latitude circle. Isoleths of constant wind speed were drawn at intervals of 100 feet of height difference over 10° of longitude (i.e., approximately at intervals of 3.7 m/sec). Five-day mean values centered one day apart were used in Fig. 2 so that the continuity of

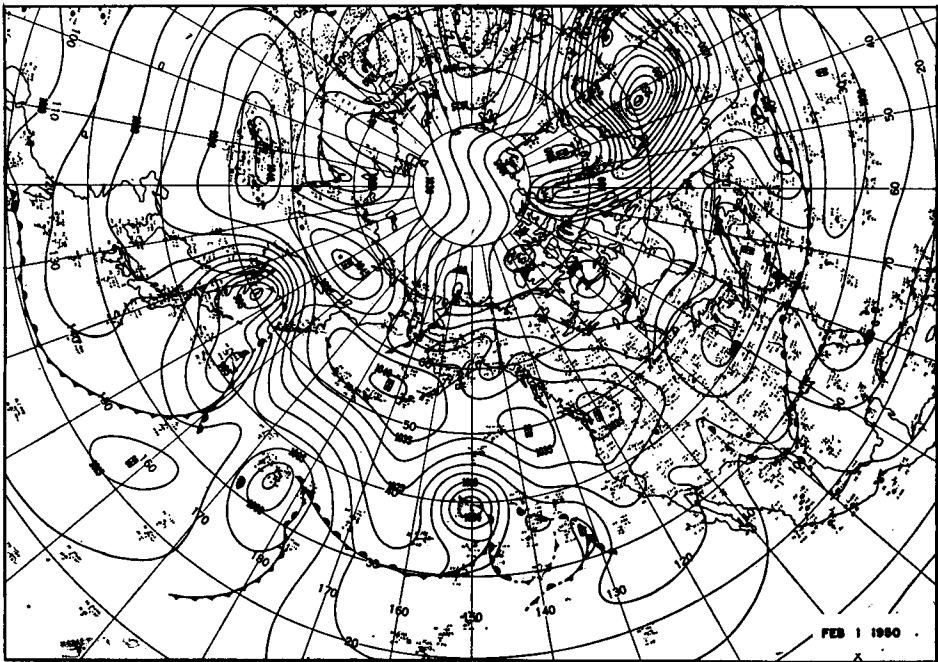
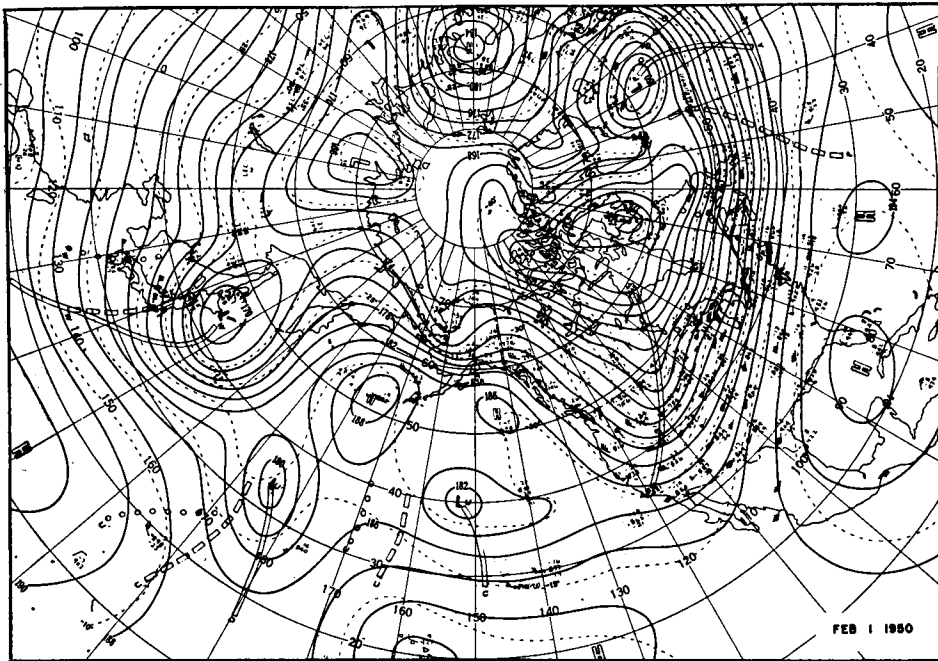
meridional flow components could be clearly established.

Of primary interest in Fig. 2 is the establishment of a new axis of southerly flow about January 30 near longitude 155° E, some 20° of longitude west of the intense southerly stream which existed from January 21 to 26. This southerly flow reached a maximum between February 2 and 3 and was subsequently followed by a maximum of northerly flow in the Gulf of Alaska (155° W) on February 5 and a maximum of southerly flow on February 6 at 125° W. This downstream progression of increasing meridional flow is similar to many other cases of what has been described as dispersion of energy through the planetary wave train at the speed of the group velocity. A clearcut case of such energy dispersion was recently treated by CARLIN (1953). Basically this phenomenon is but another way of considering the adjustments in the contour pattern associated with barotropic flux of absolute vorticity. It is apparent that from the large-scale point of view, as expressed by 5-day mean data, barotropic influences of previous developments in the upstream wave train were of considerable significance in the Gulf of Alaska trough development.

### 3. History of cyclogenesis from viewpoint of daily synoptic charts

The detailed day-to-day synoptic developments associated with this case of cyclogenesis may be found in the Daily Series of Synoptic Weather Maps of the U.S. Weather Bureau for February 1950. These maps are prepared once daily for sea level and 500 mb at 1230 G.M.T. and 1500 G.M.T., respectively. Owing to space limitations only a selected few of these charts are shown here in Fig. 3.

On January 30 and 31, 1950 (not shown) anticyclonic circulation at sea level and aloft dominated the region of Alaska, the Gulf of Alaska, and much of the Bering Sea and the Aleutians. The individual perturbation which set off the Gulf of Alaska development was located in the Bering Straits on February 1 (Fig. 3 a) and moved through Alaska into the northern Gulf by February 2 (Fig. 3 b). This system was an old occlusion which could be clearly traced from a position northwest of Kamchatka on January 30. This occlusion transformed into a cold front as it moved

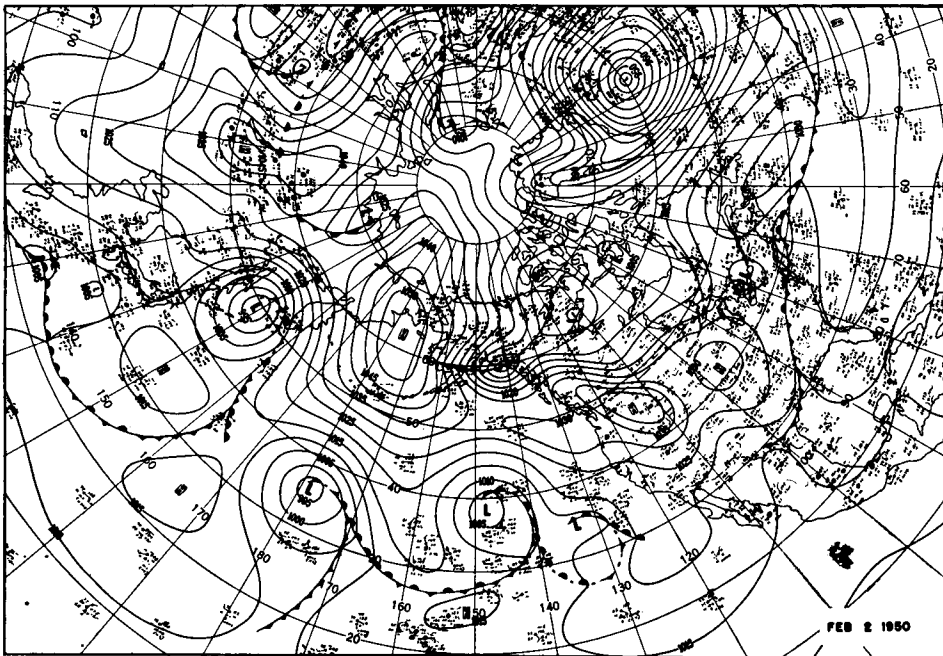
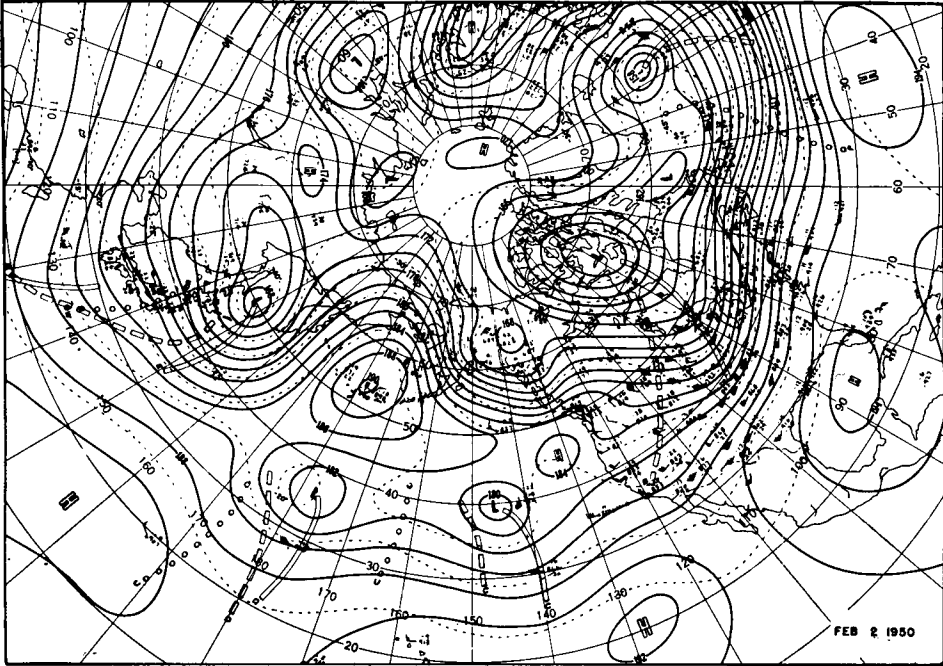


3 a

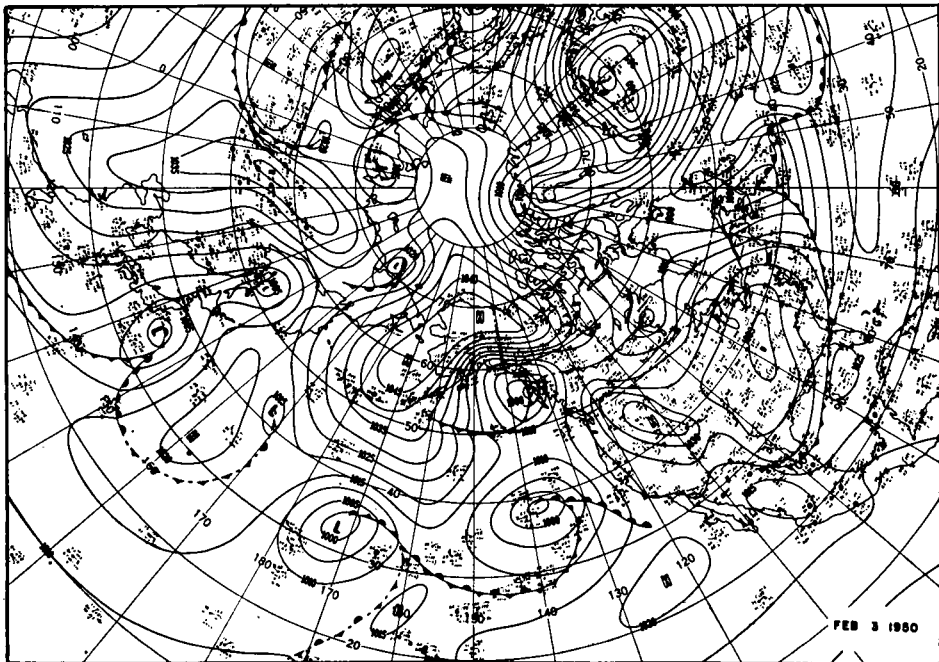
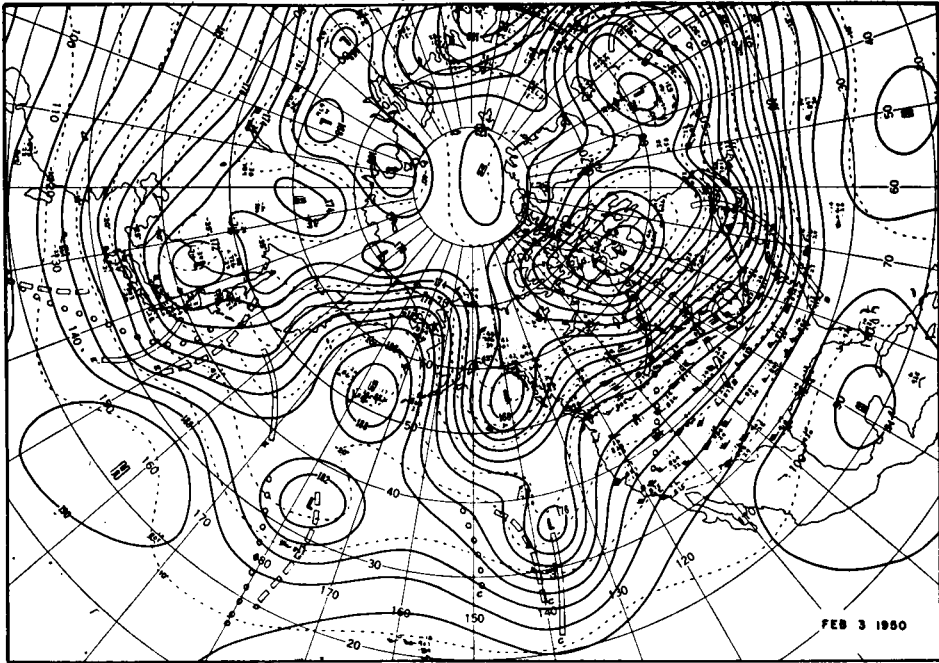
Fig. 3. Sequence of daily maps for 500 mb (upper) and sea level (lower) portraying details of cyclonic development in the Gulf of Alaska. Maps are reproductions from Daily Series Synoptic Weather Maps published by U.S. Weather Bureau. 500-mb charts are for 1500 GMT and sea-level charts for 1230 GMT.  
 3 a. February 1, 1950; 3 b. February 2, 1950; 3 c. February 3, 1950; 3 d. February 4, 1950.

Tellus VII (1955), 4

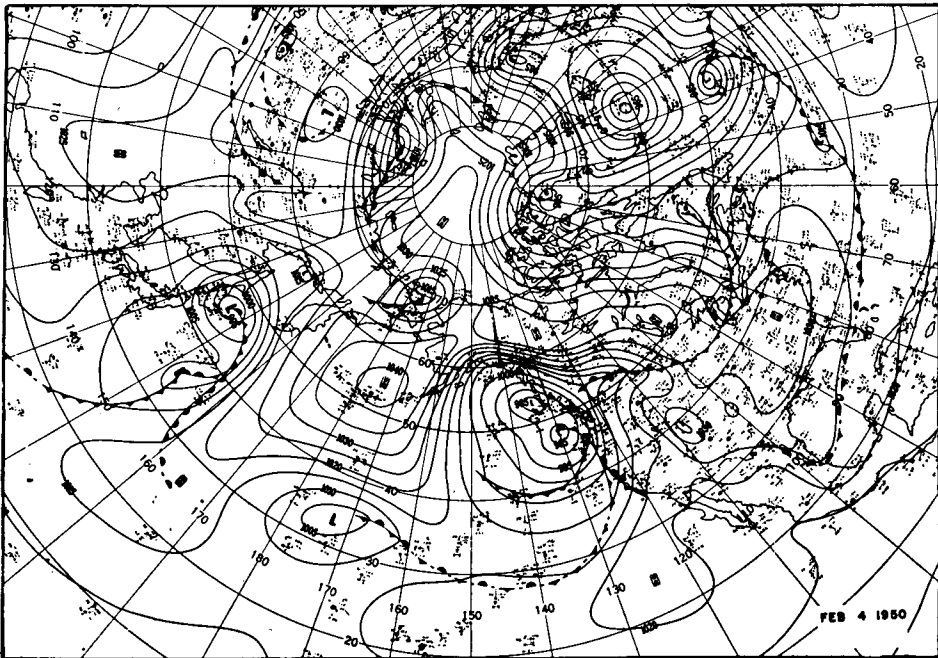
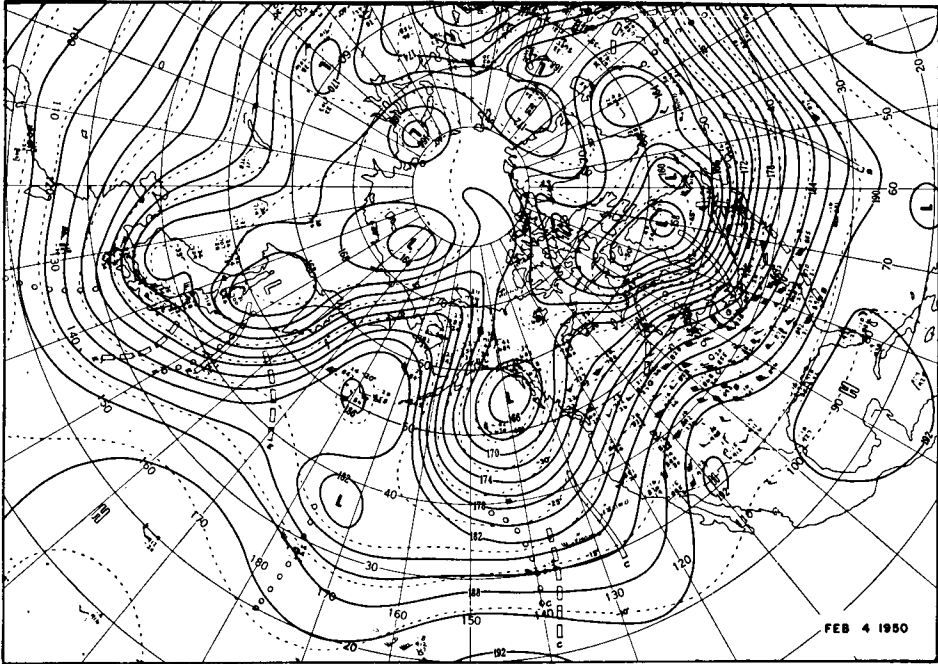
6-508697



3 b



3 c



3 d

southeastward across Alaska. Behind this front was a very cold Arctic air mass which first reached the Gulf of Alaska very close to map time of February 2 (Fig. 3 b). The intensifying cyclonic center in the northeastern Gulf at sea level formed along the front, and was not the same low which was in northwestern Alaska in Fig. 3 a. Further deepening of this new cyclone followed in the next two days (Figs. 3 c and 3 d).

At 500 mb this trough was very weak as it crossed the Bering Sea on January 31, but it began intensifying as it came into Alaska (Fig. 3 a), and a closed low center formed on February 2 (Fig. 3 b). This center drifted southward into the Gulf over the developing sea level cyclone by the next day (Fig. 3 c), and continued deepening through the next two days. The developing trough in the Gulf of Alaska extended its influence to rather low latitudes of the eastern Pacific as it became longitudinally superimposed over the pre-existing low latitude trough which had been drifting slowly eastward. This juncture of the two troughs occurred on February 3 and 4 (Figs. 3 c and 3 d) and was accompanied by deepening and northeastward motion of the low-latitude cyclone.

Rapid rises in sea-level pressure and 500-mb height had been occurring over the Aleutians, the Bering Sea, and northeast Siberia around February 1 (Fig. 3 a). These rises had been preceded on January 30 and 31 by cyclonic development near Japan (not shown) and accompanying initiation of strong southerly flow to the east of Japan at both sea level and 500 mb. The maximum intensity of the ridge over the Aleutians was reached on February 2 (Fig. 3 b) just as cyclogenesis got under way in the Gulf. Subsequently, the ridge aloft weakened slightly, but underwent little change in basic position in the next few days (Figs. 3 c and 3 d).

The events occurring on the daily charts give the same basic impression that has already been derived from inspection of the 5-day mean data (Figs. 1 and 2). This impression is that the development of a new trough in the vicinity of the Gulf of Alaska could be anticipated qualitatively from antecedent large-scale circulation changes upstream in the planetary wave pattern. Furthermore, it can also be reasonably estimated that the transmission of these influences downstream into the Gulf of Alaska was effected to

a great extent by barotropic flux of absolute vorticity. However, these deductions are as yet all qualitative. The next step is to see how much influence barotropic effects have quantitatively, and thence to estimate the relative importance of the heat source in the Gulf of Alaska.

#### 4. Barotropic tendency computations

The effects on the mid-tropospheric contour patterns due to advection of absolute vorticity alone may be measured approximately by tendency computations based on the simple barotropic form of the vorticity equation,

$$\frac{\partial \zeta}{\partial t} = - \underset{\rightarrow}{V} \cdot \nabla \eta, \quad (1)$$

where  $\zeta$  is the vertical component of relative vorticity,  $t$  time,  $\underset{\rightarrow}{V}$  horizontal wind vector,  $\nabla \eta$  the horizontal gradient of the vertical component of absolute vorticity. The absolute vorticity,  $\eta$ , is simply  $(\zeta + f)$ , where  $f$  is the Coriolis parameter. When the geostrophic approximation is made the left side of (1) can be expressed in terms of a height tendency so that we may write

$$\frac{\nabla^2 \partial z}{\partial t} = - \underset{g \rightarrow}{f} V \cdot \nabla \eta, \quad (2)$$

where  $\nabla^2$  is the horizontal Laplacian operator,  $z$  height of a constant pressure surface, and  $g$  acceleration of gravity. The right-hand side of (2) can also be expressed in terms of the height field (cf. CHARNEY, FJØRTOFT and VON NEUMANN, 1950; BOLIN and CHARNEY, 1951) and is actually evaluated in that manner, but this transformation has been omitted here for the sake of simplicity.

Equation (2) has been applied here in much the same fashion as in recent work of BOLIN and CHARNEY (1951), STAFF MEMBERS OF THE UNIVERSITY OF STOCKHOLM (1952), and ELIASSEN and HUBERT (1953). The advection of geostrophic vorticity (right side of equation 2) was computed over a square grid on a polar stereographic map projection with a grid interval of approximately 575 km at latitude  $45^\circ$ .<sup>1</sup>

<sup>1</sup> It is possible that this fairly large grid size may be somewhat too coarse to yield sufficient detail of the vorticity field. However, it is believed that the spacing between available observation stations is generally so

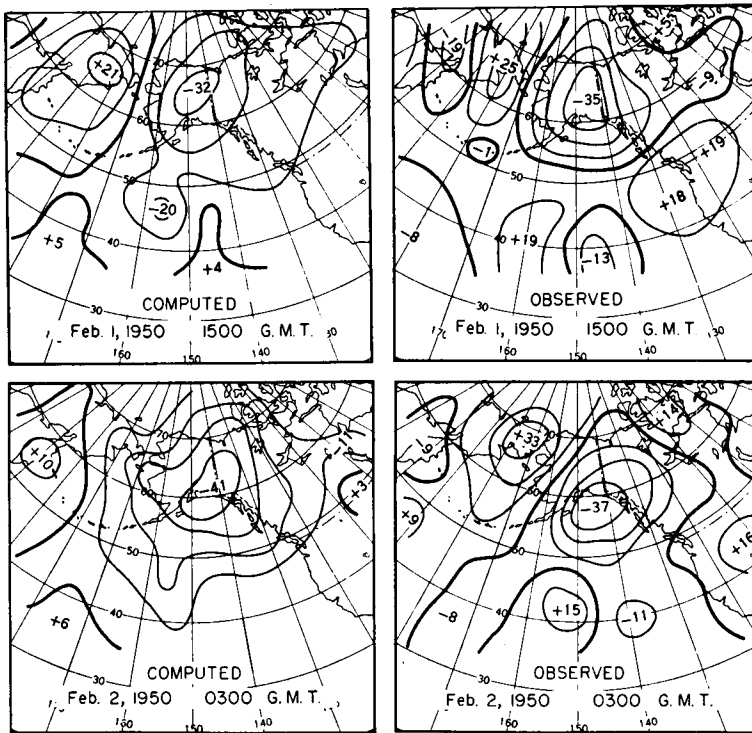


Fig. 4. Computed and observed 700-mb height changes in units of 10 ft/12 hr for early phases of Gulf of Alaska development.

The height tendencies were then determined by relaxation of this field of vorticity advection assuming that the tendencies were zero on the boundary of the area. The computational area was approximately coincident with the total region outlined in Figs. 4—6. The calculations were carried out at the 700-mb level using the twice-daily Northern Hemisphere analyses prepared by the Extended Forecast Section. The reason for the choice of the 700-mb level over the more usual 500-mb level lies mainly in the sparsity of available data over the Pacific Ocean area. Since the upper-level analysis in such regions must depend to a considerable degree upon extrapolation upward from sea-level data, it was felt that the analysis at 700 mb might be somewhat more reliable than at 500 mb. Even if upper-level data were adequate there is no conclusive

great in this case that a smaller grid might pick up spurious detail of the derivatives of the height field. This danger may exist even with the grid size used here, of course.

evidence that the 500-mb level has any basic advantages over 700 mb in regard to the application of the barotropic model. Several empirical findings (e.g., FLEAGLE, 1948; CHARNEY, 1949; PALMÉN and NEWTON, 1951) have indicated that 700 and 500 mb are about equidistant from the average level of non-divergence at which equation (2) is most applicable. It should also be mentioned that CHARNEY, FJØRTOFT, and VON NEUMANN (1950) concluded that the appropriate level lies between 500 and 400 mb. On the other hand, recent empirical data of CRESSMAN (1953) indicate that the equivalent barotropic surface is found between 650 and 600 mb. Considering all of these assorted findings it is probably safe to assume that 700 mb and 500 mb are equally amenable on the average to application of the barotropic model.

The computed barotropic tendencies are compared here with the corresponding observed 24-hour change in 700-mb height centered at the time of the map from which computations were

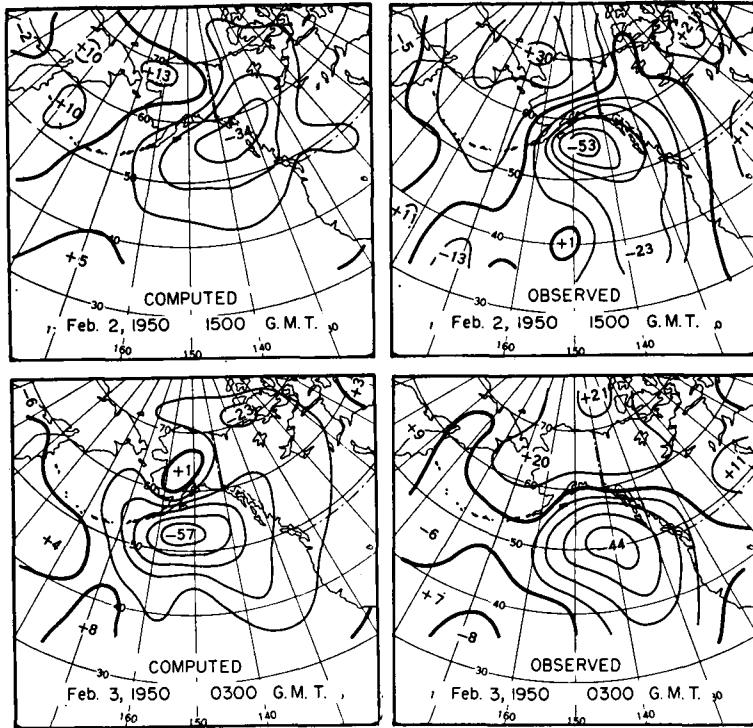


Fig. 5. Computed and observed 700-mb height changes in units of 10 ft/12 hr during periods of most rapid deepening over Gulf of Alaska.

made. It is believed that this method of comparison is somewhat preferable to that used by BOLIN and CHARNEY (1951) since their averaging of two successive 12-hour barotropic computations may automatically include some non-barotropic effects which have modified the circulation in the 12-hour interval between maps. On the other hand, the use of an observed 24-hour height change may be a somewhat poorer approximation to an instantaneous tendency than is a 12-hour change.

The results of these barotropic tendency computations as compared with observed height changes are shown in Figs. 4-6. The units in these three figures are tens of feet/12 hours. In Fig. 4 it is immediately apparent that the sizable height falls observed over Alaska and the northern Gulf of Alaska centered at 1500 G.M.T., February 1 and 0300 G.M.T., February 2 are caught fairly well by the computed barotropic tendencies. Note that the computed and observed centers of these negative height changes correspond very well in both intensity

and location. Other aspects of the agreement between computed and observed tendencies are not so good, especially over the northern Bering Sea at 0300 G.M.T. of February 2 and in both periods over the United States and near latitude  $40^{\circ}$  N over the Pacific. These errors are very likely partly attributable to boundary assumptions of zero tendencies, which can cause errors when the relaxation technique is applied.

During the next two twelve-hour periods (Fig. 5) the barotropic tendencies still call for falling heights over the Gulf of Alaska region which compare rather well with the observed tendencies. However, it is notable that the centers of maximum height fall are no longer predicted as well as in Fig. 4. At 1500 G.M.T., February 2 (Fig. 5, top) the maximum computed height fall of -34 was found along the southeast Alaskan coast while the observed height fall of -53 was located near the middle of the Gulf of Alaska. This was the time when the cold Arctic air had begun streaming out

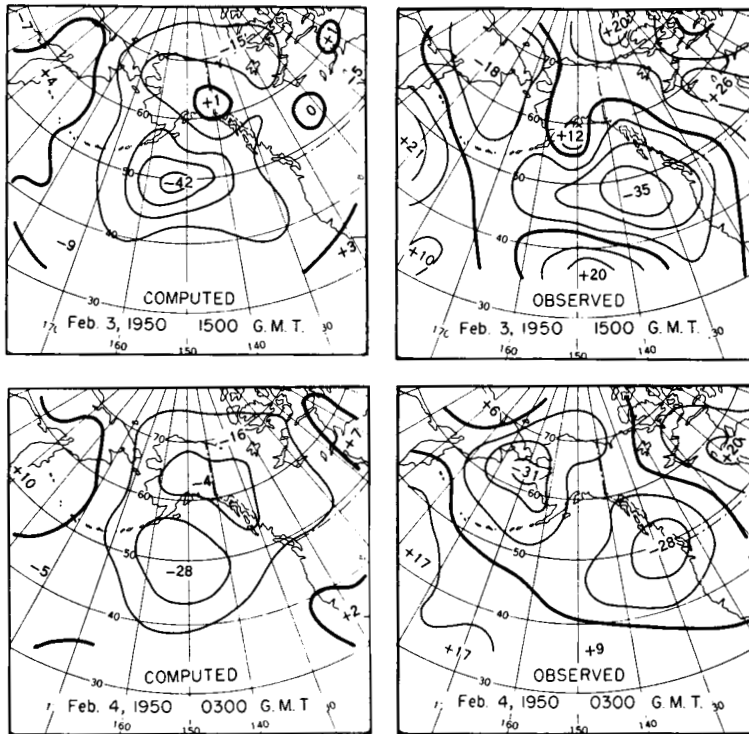


Fig. 6. Computed and observed 700-mb height changes in units of 10 ft/12 hr for two periods subsequent to rapidly deepening stage.

over the Gulf of Alaska, thereby introducing abruptly a large heat source into the atmospheric circulation. By 0300 G.M.T., February 3 (Fig. 5, bottom) a deep closed low had become established over the Gulf of Alaska at 700 mb. Barotropic computations from this flow pattern now indicated large height falls over the extreme western Gulf of Alaska, whereas the observed fall center was located considerably to the east at  $50^{\circ}$  N,  $140^{\circ}$  W and was somewhat less in central intensity. A similar discrepancy between the computed and observed fall centers was found at 1500 G.M.T., February 3 (Fig. 6, top). By 0300 G.M.T., February 4 (Fig. 6, bottom) the barotropic tendency computations had deteriorated considerably.

These computations indicate that horizontal advection of absolute vorticity was responsible for much of the cyclonic development in the Gulf of Alaska. This was especially true in the initial stages, but substantial errors in the location and intensity of the maximum height falls

began to show up at the time when cold air reached the Gulf of Alaska. In other words, simple advection of vorticity could not explain the rapidity and the exact location of the intense cyclonic development over the Gulf, but did indicate that cyclogenesis would take place in the general area. At the time of most rapid deepening the computed height falls were to the east of and weaker than the observed falls, whereas following establishment of the deep closed low computed falls were to the west and stronger than the observed falls. These errors of the barotropic computations can be attributed largely to divergence and hence to the vertical motion field. These effects will be discussed in the next section.

##### 5. Vertical motion fields associated with cyclogenesis

The importance of the vertical motion field in determining non-advective local changes in vorticity may be seen in the complete vorticity equation written in the form

$$\frac{\partial \zeta}{\partial t} = -V \cdot \nabla \eta - \omega \frac{\partial \eta}{\partial p} + \eta \frac{\partial \omega}{\partial p} + k \cdot \nabla \omega \times \frac{\partial V}{\partial p} \quad (3)$$

This equation applies to isobaric surfaces since pressure,  $p$ , has been used as the vertical co-ordinate (see ELIASSEN, 1952, for the derivation in this form). Hence,  $\nabla$  means differentiation along an isobaric surface, and  $\partial/\partial t$  represents local rate of change on an isobaric surface.  $\omega$  is the individual rate of change of pressure,  $dp/dt$ , which is essentially the vertical motion in this co-ordinate system.  $k$  is a unit vertical vector and the other symbols have the meanings given previously. In the derivation of this equation Eliassen has neglected friction and the horizontal component of the earth's rotation.

Equation (3) states then that local vorticity changes are a result of not only horizontal advection of vorticity [first term on right of (3)], but also three additional terms: vertical advection of vorticity ( $-\omega \partial \eta / \partial p$ ), divergence ( $\eta \frac{\partial \omega}{\partial p}$ ), and transformation of horizontal vorticity into vertical vorticity ( $k \cdot \nabla \omega \times \frac{\partial V}{\partial p}$ ). Although the latter term has been shown to have on occasion a relatively large magnitude (cf. REED, 1951) it was decided that it could be neglected in this case since vertical shear of the horizontal wind over the Gulf of Alaska region was generally small between 1,000 and 500 mb. If this tilting term is neglected we then have from (3)

$$\frac{\partial}{\partial p} \left( \frac{\omega}{\eta} \right) = \frac{\frac{\partial \zeta}{\partial t} + V \cdot \nabla \eta}{\eta^2}, \quad (4)$$

which upon integration becomes

$$\left( \frac{\omega}{\eta} \right)_{p_1} = \left( \frac{\omega}{\eta} \right)_{p_0} - \int_{p_1}^{p_0} \frac{\frac{\partial \zeta}{\partial t} + V \cdot \nabla \eta}{\eta^2} dp, \quad (5)$$

where  $p_1$  and  $p_0$  are arbitrary pressure surfaces. In practice  $p_0$  is assumed to be 1,000 mb and the integral is approximated by values of  $\left( \frac{\frac{\partial \zeta}{\partial t} + V \cdot \nabla \eta}{\eta^2} \right)$  at certain standard isobaric

surfaces. The vertical motion at 500 mb was obtained from the expression

$$\omega_5 = \eta_5 \left[ \left( \frac{\omega}{\eta} \right)_{10} - \frac{150}{\eta_{10}^2} \left( \frac{\partial \zeta}{\partial t} + V \cdot \nabla \eta \right)_{10} - \frac{250}{\eta_7^2} \left( \frac{\partial \zeta}{\partial t} + V \cdot \nabla \eta \right)_7 - \frac{100}{\eta_5^2} \left( \frac{\partial \zeta}{\partial t} + V \cdot \nabla \eta \right)_5 \right] \quad (6)$$

and for 700 mb by

$$\omega_7 = \eta_7 \left[ \left( \frac{\omega}{\eta} \right)_{10} - \frac{150}{\eta_{10}^2} \left( \frac{\partial \zeta}{\partial t} + V \cdot \nabla \eta \right)_{10} - \frac{150}{\eta_7^2} \left( \frac{\partial \zeta}{\partial t} + V \cdot \nabla \eta \right)_7 \right], \quad (7)$$

where the subscripts 5, 7, 10 refer to the 500, 700, and 1,000-mb surfaces respectively. In the computations it was assumed that  $\omega_{10}$  was zero, i.e., no vertical motion near ground level. This assumption is justified over the level surface areas, but is probably somewhat open to question over the mountain ranges of Alaska and western Canada. However, since the grid interval of 575 km is in many cases large enough to encompass both leeward and windward slopes of a mountain barrier  $\omega_{10} = 0$  may be the most appropriate assumption even over the mountain zones. Perhaps more restrictive over these higher elevations is the somewhat fictitious nature of the sea-level or 1,000-mb chart where substantial reductions to sea level must be made. No adjustments in equations (6) or (7) were made over these areas so that vertical motion estimates over mountainous terrain are probably somewhat less reliable than over the oceans and flatter land areas.

A few words may be in order here about the possible influence of surface friction, which is neglected in the equations. Simple assumptions about friction (cf., PANOFSKY, 1951) indicate that frictional inflow would produce upward motion at the top of the friction layer near a sea-level pressure minimum. This effect would generally enhance the upward motions calculated here near low centers and increase the downward motion near high centers. However, a recent observational study of frictional flow over an ocean surface by SHEPPARD et al. (1952) indicates that the whole classical concept of a frictional boundary layer has little validity

over the sea surface. These findings raise considerable doubt then as to whether a simple assumption of frictional inflow across isobars at the surface would have added much accuracy to vertical motion estimates made here.

In evaluating equations (6) and (7) local vorticity changes were approximated by the observed 24-hour changes centered around each given 12-hour period, while the advection of vorticity was computed from the chart at the middle of this 24-hour period. The grid used for these computations was the same as described earlier for the barotropic tendency calculations. In order to express the vertical motions in more familiar units the values of  $\omega$  were converted into the true vertical velocity  $w$ , in cm/sec through use of the hydrostatic equation. It should be pointed out by the way, especially when considering equations (6) and (7), that  $w$  is opposite in sign to  $\omega$ . The results of some of these computations of vertical motion are shown in Figs. 7—9 superimposed on the appropriate contour patterns.

Before considering some of the individual details of these vertical motions, it is of interest to point out that in general the various areas of upward and downward motion are similar in magnitude and areal extent to values calculated by other investigators in a variety of situations. This holds not only for studies where the vorticity equation was used in the calculations (e.g., SAWYER, 1949; ELIASSEN and HUBERT, 1953), but also for computations by adiabatic and kinematic methods (e. g., FLEAGLE, 1947; PANOFSKY, 1951).

Turning our attention now to Fig. 7 and concentrating on the higher latitude wave train we see that a broad area of relatively small upward motion was located in and east of the developing trough over southern and southwestern Alaska at both 700 mb and 500 mb. The maxima at both levels were over the north-eastern Gulf of Alaska. In the northwesterly flow to the rear of the trough over western Alaska and the Bering Straits pronounced downward motion occurred.

Twelve hours later (Fig. 8) upward motion continued over most of the Gulf of Alaska and became somewhat more intense. Note that these positive vertical velocities extended well back into the northwesterly flow west of the developing trough over the Gulf of Alaska at both 700 and 500 mb. The centers of maximum

upward motion were now located over the middle of the Gulf of Alaska, to the southwest of the maxima in Fig. 7, even though the trough had moved eastward. Also, the downward motion east of the ridge over western Alaska and the Bering Sea had decreased markedly from its indicated intensity twelve hours earlier.

These changes in the vertical motion distribution relative to the trough were undoubtedly associated with the deepening of the cyclonic circulation over the Gulf, but this association does not provide an explanation for these vertical motion adjustments. Rather, one must look for the cause of the vertical motion-divergence fields to get a better understanding of why rapid deepening took place in the Gulf of Alaska. Since the maximum upward motion now appeared in the northwesterly flow off the Alaskan coast (Fig. 8) and since this northwesterly flow through most of the troposphere was now carrying extremely cold air out over the Gulf of Alaska, it seems most logical to postulate that the large low-level heat source introduced in the Gulf of Alaska at this time was responsible for large-scale convergence and upward motion in this area. The mechanism for production of upward motion through heating may be attributed in simplest terms to a thermal circulation where vertical expansion of heated columns of air relative to non-heated or cooled columns leads to outflow at high levels and inflow in the lower portion of the atmosphere. This classical thermal theory of pressure change has recently been summarized by AUSTIN (1951).

In the ensuing period (Fig. 9) the vertical motion fields once more took on a more familiar appearance relative to the deep trough in the Gulf of Alaska. Generally, pronounced downward motion developed west of the trough and upward motion now dominated the area east of the trough. However, upward motion persisted in the vicinity of the trough-line itself. Positive vertical velocities also developed to the rear of the trough south of 50° N, in advance of the surface cold front. During the three subsequent 12-hour periods (not shown), fairly similar conditions prevailed, i.e., downward motion behind the trough, and upward motion ahead, as the trough moved slowly eastward.

This return to what might be considered a more typical distribution of vertical motion

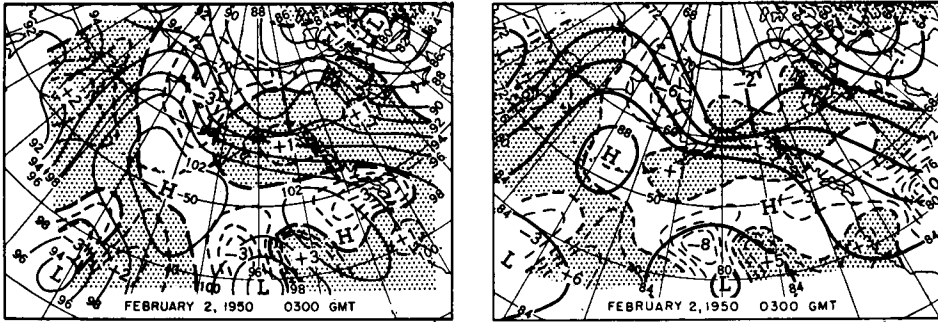


Fig. 7. Vertical motion (in cm/sec) at 700 mb (left) and 500 mb (right) for 0300 GMT, February 2, 1950. Shaded areas indicate upward motion, unshaded areas downward motion. Dashed isopleths of vertical motion are drawn at intervals of 1 cm/sec at 700 mb and 2 cm/sec at 500 mb. Contours of 700-mb surface are drawn for every 200 ft while 500-mb contours are at intervals of 400 ft.

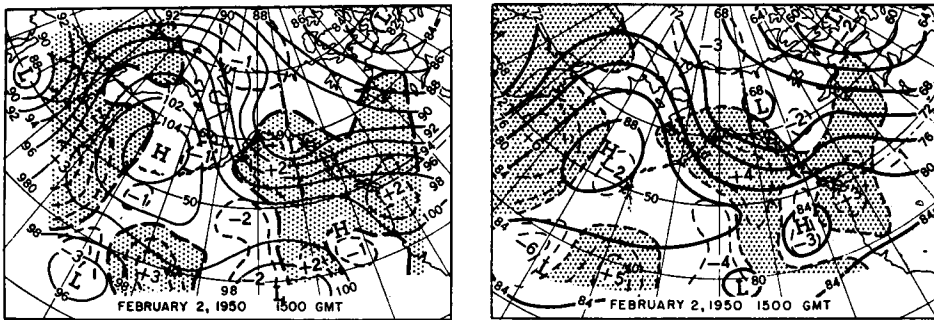


Fig. 8. Vertical motion (in cm/sec) at 700 mb (left) and 500 mb (right) for 1500 GMT, February 2, 1950. See legend to fig. 7.

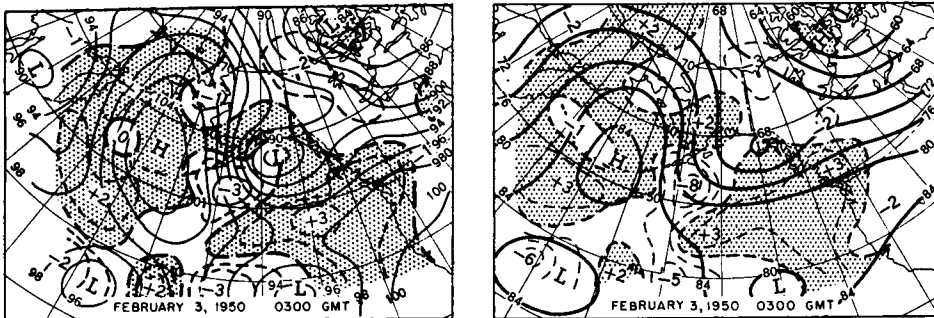


Fig. 9. Vertical motion (in cm/sec) at 700 mb (left) and 500 mb (right) for 0300 GMT, February 3, 1950. See legend to fig. 7.

relative to the trough in the Gulf of Alaska seems to imply that the usual effects of subsidence and horizontal divergence of the cold air mass in its southward drift, and lifting and horizontal convergence of the warmer air mass east of the trough once again became dominant  
Tellus VII (1955), 4

even though a pronounced heat source still existed as cold air continued to stream out over the Gulf. Thus, the tentative conclusion one can draw from this series of vertical motion computations (and also from the essentially dependent barotropic tendency computations)

is that the effects of heating in this cyclogenetic development were most influential during a relatively short period (i.e., of the order of some 12–24 hours) following the initial establishment of the heat source. After the cold dome moved out over the ocean in greater depth, both horizontally and vertically, the more powerful effects of sinking and spreading of the cold air counteracted the convergence effects of heating from the ocean surface.

## 6. Calculations of atmospheric heating in the Gulf of Alaska

In view of the apparent influence of heating in Gulf of Alaska cyclogenesis, it is important to obtain some quantitative information about the amount of heat added to the air in this situation. In fact, if the heating could be specified *a priori* in some simple functional form, it would be feasible to include heating effects in current numerical forecasting techniques (e.g., CHARNEY and PHILLIPS, 1953). As yet there does not seem to be any practical way of writing down the true heating function, but empirical studies of heating may provide the basis for some approximate heating model in certain specific cases. In regard to the particular problem of heating of cold air masses over the sea, with which we are primarily concerned in the case of Gulf of Alaska cyclogenesis, there have been several pertinent studies. JACOBS (1951) calculated sensible heat exchange between ocean and atmosphere from long-term average values of differences between sea and surface air temperatures. WEXLER (1944) and MÖLLER (1950) determined normal regions of heating from mean circulation data, while AUBERT and the present author (1951) calculated heating in similar fashion for individual months. Studies of heating of Polar or Arctic air in its passage over the North Atlantic have been made by BURKE (1945) and KLEIN (1946) and more recently by CRADDOCK (1951). There have also been similar studies of air mass heating over other water bodies such as Hudson Bay (BURBIDGE, 1951). Except for Jacobs' work all of these studies have suffered (aside from practical computational difficulties in the techniques used) from their inability to separate adiabatic warming and cooling from the true heat sources. In the heating calculations made here vertical motions obtained in the previous section have been applied to yield what, it is

hoped, is a better approximation to the true non-adiabatic heating of the air.

The heating of a layer of air may be expressed as

$$\left(\frac{dQ}{dt}\right)_L = \frac{c_p \Delta p}{g} \frac{d\bar{\vartheta}}{dt} = \frac{c_p \Delta p}{g} \left(\frac{\delta\bar{\vartheta}}{\delta t}\right)_p + \frac{c_p \Delta p}{g} \frac{\omega \partial \bar{\vartheta}}{\partial p} = H + V. \quad (8)$$

Here,  $\left(\frac{dQ}{dt}\right)_L$  is the rate at which heat is added to a square centimeter column of depth  $L$ ,  $\vartheta$  is potential temperature,  $c_p$  specific heat at constant pressure,  $\Delta p$  pressure difference between top and bottom of layer under consideration.  $\left(\frac{\delta\bar{\vartheta}}{\delta t}\right)_p$  is the change of potential temperature following an isobaric trajectory. The bars represent vertical averages through the layer. Other terms have meanings previously defined.  $H$  and  $V$  have been introduced as shorthand notations for heating measured by temperature change in the horizontal trajectory of the air and heating measured by the vertical advection of potential temperature, respectively.

Isobaric trajectories were constructed on the 1,000, 850, 700, and 500-mb surfaces originating at Anchorage, Alaska, which was generally located near the middle of the stream of cold air pouring out of Alaska. In constructing these trajectories the geostrophic wind field on a particular map was considered to be representative of the flow field for a period of twelve hours centered at map time. An example of these computed trajectories is given in Fig. 10. Temperatures were interpolated from analyzed temperature fields at each of the pressure surfaces at the end of 12 (dots) and 24 hours (arrow heads). These temperature readings were then used to construct two "synthetic" soundings for 12 and 24 hours later which when compared with the original observed sounding at Anchorage showed the amount of heating of the air column as it moved in its isobaric trajectory. An example of the initial sounding as compared with "synthetic" soundings is also shown in Fig. 10.

As exemplified by Fig. 10 the trajectories at the various levels had diverged considerably by the end of 24 hours, but were fairly close together at the end of the first 12 hours. Since the assumption that we are following a vertical

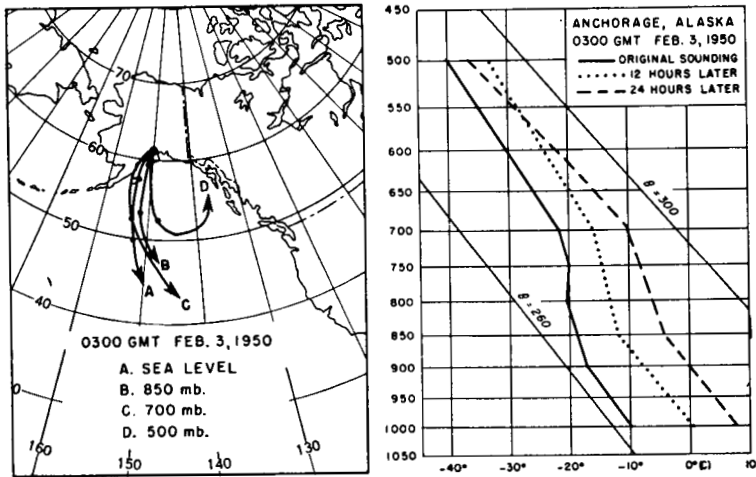


Fig. 10. Example showing trajectories and soundings used in arriving at heating calculations (term  $H$  of equation 8) Computed trajectories originating from Anchorage, Alaska at 0300 GMT, February 3 for four indicated isobaric surfaces are shown at left. Dots along paths indicate positions of air parcels after 12 hours and arrow heads show positions at the end of 24 hours. Pseudo-adiabatic chart at right shows initial sounding at Anchorage and »synthetic« soundings 12 and 24 hours later obtained from temperatures interpolated from isotherms on analyzed constant pressure charts at indicated points on trajectories.

column of air is tenuous at best, it was considered that reliable computation of  $H$  (see equation 8) could be carried out only for the first 12 hours of the air's travel southward from Anchorage. The vertical term ( $V$  of equation 8) was estimated from the average vertical motions (as calculated in the previous section) and the average vertical gradient of potential temperature along the trajectories. These heating calculations for five twelve-hour periods starting shortly after the cold air first broke out in force over the Gulf of Alaska are shown in Table 1.

Of considerable significance in this table are the large magnitudes of the total heating in the layer from 1,000 to 500 mb. These estimates include the effects of all heat sources of course, but it is fairly certain that the greater part of

this heating is due to sensible heat gain from the ocean surface. Comparison of these figures with normal daily heating for winter (cf., Fig. 59, JACOBS, 1951) shows that the maximum daily heating observed here is an order of magnitude greater than normal for the Gulf of Alaska region and more than five times as great as the maximum normal heating found at any point in the Northern Hemisphere. However, the heating calculations of Table 1 agree fairly well with those of CRADDOCK (1951) who studied similar air-mass heating following trajectories in the northeastern Atlantic. At any rate these figures emphasize that there is little doubt that sensible heating of air from the sea surface is the most potent atmospheric heat source that is encountered on a relatively large scale.

Table 1. Heating of air associated with cyclogenesis in the Gulf of Alaska, February 2-4, 1950 as calculated using equation (8). Subscripts 7-10, 5-7, and 5-10 refer to layers 700-1,000 mb, 500-700 mb, and 500-1,000 mb, respectively. Units are ly/day

12-Hour Period Beginning	$H_{7-10}$	$V_{7-10}$	$\frac{dQ}{dt}_{7-10}$	$H_{5-7}$	$V_{5-7}$	$\frac{dQ}{dt}_{5-7}$	$\frac{dQ}{dt}_{5-10}$
1500 GMT, Feb. 2 . . . . .	+ 1,100	+ 170	+ 1,270	+ 590	+ 350	+ 940	+ 2,210
0300 GMT, Feb. 3 . . . . .	+ 1,190	- 170	+ 1,020	+ 700	- 290	+ 410	+ 1,430
1500 GMT, Feb. 3 . . . . .	+ 1,050	- 200	+ 850	+ 550	- 310	+ 240	+ 1,090
0300 GMT, Feb. 4 . . . . .	+ 840	- 140	+ 700	+ 50	- 230	- 180	+ 520
1500 GMT, Feb. 4 . . . . .	+ 600	- 100	+ 500	+ 100	- 200	- 100	+ 400

As might be expected from the nature of the heat source the greater part of the heating is found in the layer below 700 mb, but the contribution in the layer 700 to 500 mb is by no means negligible. Since sensible heating from the sea is concentrated at the surface, turbulent vertical exchange up to rather high levels of the troposphere must account for much of the sizable values of heating found in the upper layer during the first three periods. It is also likely that the release of heat of condensation contributes to this heating at these levels as well as below 700 mb.

Table 1 shows also that the contributions of net vertical advection of potential temperature,  $V$ , to the total heating,  $dQ/dt$ , are of relatively little importance (although not negligible) in the layer 1,000 to 700 mb while the horizontal term,  $H$ , is large. However, as  $H$  becomes smaller  $V$  takes on an increasing relative importance. In the layer 700 to 500 mb  $V$  is generally of equal importance as compared with  $H$  since the former is generally larger as one goes aloft while the latter becomes smaller. Thus, during the last two periods  $V$  becomes dominant between 700 and 500 mb and net cooling is indicated in the layer. Cooling of the order of 100—200 ly/day can very likely be attributed to radiation.

The calculations point very clearly to the fact that heating over the Gulf reaches its peak immediately after the cold air outbreak and decreases in intensity in the ensuing periods. This is probably due to the setting in of subsidence which restricts vertical turbulent transfer mainly to lower tropospheric layers.

The data in Table 1 may be drawn upon to demonstrate the importance of considering heating in numerical prediction models. In baroclinic models the first law of thermodynamics [equation (8)] has been used as the second prediction equation in order to take care of the unmeasurable divergence term in the vorticity equation [equation (4)]. In these models the adiabatic assumption has generally been made, i.e.,  $\frac{dQ}{dt} = 0$ . If this is done in (8) "adiabatic" vertical motion can be calculated as follows:

$$\bar{\omega}_A = -\frac{(\bar{\delta\theta/\delta t})_p}{\partial\theta/\partial p}. \quad (9)$$

Vertical motions along the trajectories calculated by this adiabatic method are given in Table 2. These are compared with the corresponding vertical motions which were obtained from the vorticity equation in the preceding section and which were used to evaluate the vertical terms ( $V$ ) in Table 1.

Table 2. Comparison of vertical motions determined from the vorticity equation ( $w$ ) with vertical motions obtained by making the adiabatic assumption  $w_A$ . These vertical velocities are averages for the layers 700—1,000 mb and 500—700 mb and for 12-hour isobaric trajectories originating at Anchorage. These were derived from data of Table 1. Units are cm/sec (positive sign indicates upward motion)

12-Hour Period Beginning	700—1,000 mb		500—700 mb	
	$w$	$w_A$	$w$	$w_A$
1500 GMT, Feb. 2	+ 0.5	— 3.3	+ 1.8	— 3.1
0300 GMT, Feb. 3	— 0.5	— 3.6	— 1.5	— 3.6
1500 GMT, Feb. 3	— 0.7	— 3.7	— 1.7	— 3.0
0300 GMT, Feb. 4	— 0.6	— 3.6	— 1.7	— 0.4
1500 GMT, Feb. 4	— 0.5	— 3.1	— 1.4	— 0.7

The most striking fact shown in Table 2 is that the adiabatic assumption in this case would have generally led to values of vertical motion markedly in error, presuming that those computed diagnostically from the vorticity equation were much closer to the truth. The adiabatic assumption would have been especially bad in the first period since strong downward motion would have been indicated when upward motion actually occurred. At this time the error was greater in the layer 700—500 mb than in the 700—1,000 mb layer. In the other periods the error was not as great, but it was consistently greater in the layer below 700 mb than in the layer above 700 mb. These differences in vertical motion indicate that baroclinic models neglecting non-adiabatic heating would very likely have yielded rather poor results in the prediction of this cyclogenesis, especially during the early stages of rapid deepening and in the lower layers during the later stages of development.

## 7. Conclusion

In summary, the following mechanism is indicated for Gulf of Alaska cyclogenesis of the type studied in this case:

1. The development is initiated largely by barotropic flux of absolute vorticity as a result of antecedent upstream readjustments in the planetary wave pattern. The upstream ridge shifts far enough west so that a new broad stream of northerly flow is established. This northerly flow transports a deep layer of extremely cold air out over the Gulf of Alaska.

2. As this cold air travels over the open waters of the Gulf it is heated at a rate of as much as 2,000 ly/day in the layer from sea level to 500 mb. Large-scale convergence and upward motion develop in the lower and middle troposphere in the region of this newly established heat source. This convergence creates new cyclonic vorticity and hence rapid deepening of the cyclone center and the associated trough. Most of the major circulation changes occur in the short period of less than 24 hours. Even in this stage, however, barotropic vorticity advection still accounts for a considerable part of the deepening.

3. Following this rapid transition in the circulation pattern further deepening occurs, but vorticity changes and vertical motion are more in accord with the usual dynamics of large-amplitude waves.

These findings raise the question as to whether heating effects of large magnitude can be neglected in short period forecasting by dynamical methods any more than they can be in extended period forecasting. A definitive answer to this question can only be obtained

by testing complex baroclinic numerical forecasting models (both including and excluding heat sources) on situations where large heat sources exist. If heating proves to be of major importance, some substantially improved means of calculating the distribution of heating independently of the field of motion must be devised. This goal may indeed be unattainable in the near future since the circulation and heat sources are so closely and complexly interdependent and since knowledge of the physical processes involved in turbulent transfer of heat, condensation and evaporation, radiation, and conversion of energy is so meager. The alternative may well be some empirical method of incorporating heat sources based on extensive observational programs which would attempt to determine atmospheric heating associated with various types of flow patterns, thermal distributions, and geographical features.

#### 8. Acknowledgments

The author wishes to express his gratitude to Mr J. Namias for suggesting this study of Gulf of Alaska cyclogenesis and his continuing interest in the work. The encouragement and helpful advice of Mr Philip F. Clapp in many phases of this study are sincerely appreciated. Thanks are also due Mr R. A. Green for his careful assistance in analysis of data and Mrs Mildred Matthews for her aid in the laborious computations.

#### REFERENCES

- AUBERT, E. J., and WINSTON, J. S., 1951: A study of atmospheric heat-sources in the northern hemisphere for monthly periods. *J. Meteor.*, **8**, 111—125.
- AUSTIN, J. M., 1951: Mechanism of pressure change. *Compendium Meteor.*, Boston, Amer. Meteor. Soc., 630—638.
- BOLIN, B., and CHARNEY, J. G., 1951: Numerical tendency computations from the barotropic vorticity equation. *Tellus*, **3**, 248—257.
- BURBIDGE, F. E., 1951: The modification of continental polar air over Hudson Bay. *Quart. J. R. meteor. Soc.*, **77**, 365—374.
- BURKE, C. J., 1945: Transformation of polar continental air to polar maritime air. *J. Meteor.*, **2**, 94—112.
- CARLIN, A. V., 1953: A case study of the dispersion of energy in planetary waves. *Bull. Amer. meteor. Soc.*, **34**, 311—318.
- CHARNEY, J. G., 1949: On a physical basis for numerical prediction of large-scale motions in the atmosphere. *J. Meteor.*, **6**, 371—385.
- CHARNEY, J. G., FJØRTOFT, R., and VON NEUMANN, J., 1951: Numerical integration of the barotropic vorticity equation. *Tellus*, **2**, 237—254.
- , and PHILLIPS, N. A., 1953: Numerical integration of the quasi-geostrophic equations for barotropic and simple baroclinic flows. *J. Meteor.*, **10**, 71—99.
- CRADDOCK, J. M., 1951: The warming of arctic air masses over the eastern North Atlantic. *Quart. J. R. meteor. Soc.*, **77**, 355—364.
- CRESSMAN, G. P., 1953: An application of absolute-vorticity charts. *J. Meteor.*, **10**, 17—24.
- ELIASSEN, A., 1952: Simplified models of the atmosphere designed for the purpose of numerical weather prediction. *Tellus*, **4**, 145—156.
- , and HUBERT, W. E., 1953: Computation of vertical motion and vorticity budget in a blocking situation. *Tellus*, **5**, 196—206.
- FLEAGLE, R. G., 1947: The fields of temperature, pressure, and three-dimensional motion in selected weather situations. *J. Meteor.*, **4**, 165—185.

- FLEAGLE, R. G., 1948: Quantitative analysis of factors influencing pressure change. *J. Meteor.*, **5**, 281—292.
- JACOBS, W., 1951: The energy exchange between sea and atmosphere and some of its consequences. *Bull. Scripps Inst. Oceanog. Univ. Cal.*, **6**, 27—122.
- KLEIN, W. H., 1946: Modification of polar air over water. *J. Meteor.*, **3**, 100—101.
- MÖLLER, F., 1950: Die Wärmebilanz der freien Atmosphäre im Januar. *Meteor. Rundschau*, **3**, 97—108.
- NAMIAS, J., and CLAPP, P. F., 1944: Studies of the motion and development of long waves in the westerlies. *J. Meteor.*, **1**, 57—77.
- PALMÉN, E. and NEWTON, C. W., 1951: On the three-dimensional motions in an outbreak of polar air. *J. Meteor.*, **8**, 25—39.
- PANOFSKY, H., 1951: Large-scale vertical velocity and divergence. *Compendium Meteor.*, Boston, Amer. Meteor. Soc., 639—646.
- REED, R. J., 1951: A study of atmospheric vorticity. Tech. Rpt. No. 10, *Research on atmospheric pressure changes*, M. I. T., 20 pp.
- SAWYER, J. S., 1949: Large scale vertical motion in the atmosphere. *Quart. J. R. meteor. Soc.*, **75**, 185—188.
- SHEPPARD, P. A., CHARNOCK, H., and FRANCIS, J. R. D., 1952: Observations of the westerlies over the sea. *Quart. J. R. meteor. Soc.*, **78**, 563—582.
- SMAGORINSKY, J., 1953: The dynamical influence of large-scale heat sources and sinks on the quasi-stationary mean motions of the atmosphere. *Quart. J. R. meteor. Soc.*, **79**, 342—366.
- STAFF MEMBERS, UNIVERSITY OF STOCKHOLM, 1952: Preliminary report on the prognostic value of barotropic models in the forecasting of 500 mb height changes. *Tellus*, **4**, 21—30.
- SUTCLIFFE, R. C., 1947: A contribution to the problem of development. *Quart. J. R. meteor. Soc.*, **73**, 370—383.
- WEXLER, H., 1944: Determination of the normal regions of heating and cooling in the atmosphere by means of aerological data. *J. Meteor.*, **1**, 23—28.